The Cryosphere Discuss., 9, 2709–2744, 2015
www.the-cryosphere-discuss.net/9/2709/2015/
doi:10.5194/tcd-9-2709-2015

The Cryosphere Discussions
Open Access

Correction of albedo measurements due to unknown geometry

U. Weiser[1], **M. Olefs**[1], **W. Schöner**[2], **G. Weyss**[1], **and B. Hynek**[1]

[1]Central Institute for Meteorology and Geodynamics, Vienna, Austria
[2]Institute of Geography and Regional Research, University of Graz, Graz, Austria

Received: 16 February 2015 – Accepted: 14 April 2015 – Published: 7 May 2015

Correspondence to: U. Weiser (ursula.weiser@zamg.ac.at)

Published by Copernicus Publications on behalf of the European Geosciences Union.

Abstract

The diurnal albedo variation of glaciers on clear sky days can be relatively high due to geometric effects induced by tilt errors. In the present paper, these tilt errors of albedo measurements are corrected in cases where tilts of both, the sensors and the slopes are not accurately measured. For this method of correction, a nearby reference measurement with a horizontally levelled sensor is needed to determine atmospheric parameters. Based on that a model is developed that is fitted to the measured data to determine tilts and directions of sensors and slopes, which vary daily due to changing atmospheric conditions and snow cover. Once these parameters are determined, the albedo, the radiative balance and the energy balance can be corrected. The differences between measured and corrected values show an obvious under- or overestimation of albedo, depending on the direction of the slope. It is also demonstrated that the difference between measured and corrected albedo is highest for high solar zenith angles.

1 Introduction

Reflected solar radiation and hence the energy balance of snow and ice surfaces strongly depend on snow albedo. The energy balance of a glacier surface defines the amount of energy available for the ablation processes, once the underlying snow/ice is isothermal.

In isolated areas of many glaciers it is difficult to make permanent manual reference measurements of tilts and directions of sensors and slopes. This means that the geometry of the measurement site is unknown because of changing physical conditions, inclinations of sensors and changing snow cover. Accurate tilt measurements only make sense when the direction of the radiation sensor is known (ideally southwards) which is not always possible due to changing conditions.

In the method described in this paper, measurement errors due to the cosine law as well as other measurement errors and uncertainties are considered.

Many publications note that tilt errors in albedo measurements can be several 100 % when the sun is low in the sky, especially on snow and glacier surfaces. Large deviations from the expected true diurnal albedo occur due to non horizontally levelled sensors.

In a paper investigating spectral reflected radiation on glacier surfaces, Dirmhirn and Eaton (1975) mention tilt errors of albedo measurements which lead to under- and over-estimations caused by the specular components of daily albedo. The focus of that paper was spectral reflected radiation that varies continuously over time and increases with the number of melting and refreezing processes. Dirmhirn and Eaton (1975) concluded that incoming shortwave radiation dominated by the direct component is underestimated at low sun angles due to the cosine measurement error (due to imperfections of the glass dome and the reflection properties of the sensor's black paint, Muneer, 1997) leading to an underestimation of global radiation at low sun angles and thus overestimating albedo. Also, the direct sun beam, which is the main part of global radiation on clear sky days, and instrumental error due to cosine law cannot be separated. These errors can be minimized by using instruments with small opening angles and deriving the albedo via spatial integration. Dirmhirn also mentioned difficulties in albedo measurement over non horizontal surfaces and suggested eliminating this problem by using horizontal and uniform surfaces with instruments close to the ground.

Sicart et al. (2001) and Oerlemans (2010) described problems of albedo measurements on tilted surfaces, but assumed a horizontally levelled pyranometer and directly measured tilts and directions of the slope to correct albedo values.

Landry et al. (2007) described the influence of both, a tilted slope and an inclined pyranometer, on albedo measurements. They corrected the albedo values by using directly measured tilts and directions.

Ineichen et al. (1987) and Schaaf et al. (1994) described the radiation on a tilted area without snow cover, measured by an inclined pyranometer with known tilts. Measurement with a horizontally levelled pyranometer over a horizontal area served as a comparison. The results showed an apparent diurnal variation of albedo over a forest surface, even the diurnal average albedo showed differences between tilted and horizontal measurements. These results are essential because albedo of a forest is expected to be almost constant, in contrast to snow albedo which changes over time.

Allen et al. (2006) used a model of solar radiation on tilted surfaces and integrated analytically over one day, also considering the extinction through the atmosphere. This model was compared to measurements above surfaces with similar tilts and directions, where relative humidity, aerosols and other meteorological influences were considered. By this comparison they estimated the extinction coefficient as a function of the measured atmospheric parameters. Furthermore, the irradiance on tilted surfaces based on horizontal measurements was modeled. As opposed to the method described in the following, no horizontal reference measurement was used to estimate the extinction through the atmosphere.

Mannstein (1985) described a method where tilts and directions of slopes were estimated from the data of the down-facing pyranometer using the measured albedo on preceding clouded day. That paper was used to verify the method described herein (Weiser, 2012), as tilts and directions were unknown. Since the paper did not consider that albedo on clouded days is approximately 0.15 higher compared to clear sky days due to the change in the spectral composition of the incoming radiation (Oerlemans, 2010), applying this method can lead to high inaccuracy.

With the method described in the present paper, albedo can be estimated from the measured data where tilts and directions of both the slope and the sensor are unknown and a horizontally levelled pyranometer is available in proximity to the measuring site. In contrast to other methods, a model for albedo measurement is developed and fitted to the measured data, considering atmospheric parameters, such as extinction coefficient and the diffuse part of global radiation. Tilts and directions of both the slope and the

TCD
9, 2709–2744, 2015

sensor are derived thereof. Using this method, the measured diurnal albedo can be corrected with high accuracy as will be demonstrated in the following sections.

2 Methods

2.1 Albedo over snow and ice surfaces

Snow albedo (α) is part of the radiative balance (Eq. 27) which in turn, is part of the energy balance that acts as an indicator for the energy available for melting processes of a glacier.

Albedo in general is derived from global and reflected solar radiation measured with a levelled pyranometer by dividing the values of the down-facing sensor ($F^{\uparrow}$, reflected radiation) by those of the up-facing sensor ($F^{\downarrow}$, global radiation):

$$\alpha(t) = \frac{F^{\uparrow}(t)}{F^{\downarrow}(t)} \quad (1)$$

Typically, daily average snow albedo is expected to decrease in periods without snowfall due to metamorphism of the snow cover, such as melting and refreezing processes.

However, on clear sky days measured albedo values show a strong diurnal variation often exceeding the realistic physical range, depending on tilts and directions of slopes and sensors and especially shortly after sunrise and before sunset due to the cosine error of the sensors. The surface geometry of a snow cover changes continuously and the tilts of the sensors increase over time, due to the fact that the automatic weather stations (AWS) are drilled into the glacier. Hence, it makes sense to manually adjust tilts and directions on a daily basis to estimate reasonable diurnal mean albedo values.

The method described in the present paper shows how to correct the true albedo with unknown tilts and directions of both the slope and the sensor.

Using a model that simulates the direct incoming radiation being reflected diffusely from a tilted surface, the slope of the observed apparent diurnal variation of albedo can be reproduced. To obtain an accurate estimation of the actual albedo when tilts and directions of the slope are unknown, the model is improved and compared to the measured data by fitting the parameters of the model to the measured data, also considering atmospheric parameters.

2.1.1 Albedo measurements

Albedo measurements are conducted with two opposite pyranometers (albedometer), one facing the upper hemisphere measuring the incoming radiation $F^{\downarrow}$, the other one facing the lower hemisphere measuring the reflected radiation $F^{\uparrow}$.

A pyranometer consists of a thermopile with black coating, absorbing the total solar radiation. The sensors have a glass cover that is transparent defining the exact spectral range and to protect the sensing elements. Radiation is absorbed in the thermopile, producing a voltage output by differential heating.

The used sensors are Kipp & Zonen CNR4 "Net Radiometer" measuring all four radiation components (incoming shortwave radiation SW_{in}, reflected shortwave radiation SW_{out}, incoming longwave radiation LW_{in}, reflected longwave radiation LW_{out}) using separate sensors within the same housing, so all radiation measuring sensors are tilted equally. For an opening angle of 160° the cosine error of the "Net Radiometer" is given as $< 5\,\%$ by the manufacturer. The uncertainty of the pyranometer indicates $<$ $4\,\%$ within a temperature range of $-10\,^{\circ}\mathrm{C} < T < 40\,^{\circ}\mathrm{C}$ and $4\,\%$ for $T \leq -10\,^{\circ}\mathrm{C}$.

The "Net Radiometers" are part of the automatic weather stations (AWS) on the two Sonnblick glaciers Goldbergkees (GOK) and Kleinfleißkees (FLK), measuring also air temperature, wind speed and direction, relative humidity and air pressure to determine mass- and energy balance of the glaciers. A solar panel serves as power supply for the AWS.

A MEAS DQG-Series conductometric dual axis inclinometer is attached to each AWS. Four oppositely polarized electrodes are dipped into an electrolytic fluid, producing a voltage that is measured. The conductivity of the electrolyte depends on its depth. When the sensor is tilted, the depth of the electrolyte and consequently its

TCD
9, 2709–2744, 2015

conductivity changes. The uncertainty of the inclinometer is 0.5 % within a temperature range of $-40^{\circ}\mathrm{C} < T < 85^{\circ}\mathrm{C}$. To use the data of the inclinometer it is necessary to know the orientation of one axis (e. g. southwards). Due to the mounting of the AWS on the glaciers, the orientation of the sensors changes continuously and is therefore estimated with an uncertainty of ±5 %.

One, ten and sixty minute average output values of all sensors connected to the AWS are stored.

To determine the optical properties of the atmosphere for the incoming solar radiation, data from a Suntracker, which is part of the Baseline Surface Radiation Network (BSRN), is used. The Suntracker is equipped with two Kipp & Zonen CMP 21 pyranometer and one Kipp & Zonen CGR 4 pyrgeometer next to each other with opening angles of 180°. The tracker follows the sun to shadow one of the pyranometers in order to measure global and diffuse radiation.

Figure 1 and Table 1 show the geographic parameters of the employed measurement stations, Suntracker on Sonnblick Observatory (SBO), AWS Kleinfleißkees (FLK), AWS Goldbergkees (GOK) and Central Institute for Meteorology and Geodynamics (ZAMG) in Vienna, Hohe Warte 38 (WHW).

The described method was tested with a measurement setup on the roof of ZAMG (WHW), over a concrete surface. To determine the exact and presumably constant albedo of the concrete, the pyranometer was levelled horizontally. In the literature, albedo over a concrete surface is given by $\alpha_{\mathrm{concrete}} = 0.17$–$0.27$ (Santamouris, 2006).

2.2 Model for solar radiation on a tilted surface

2.2.1 Radiation model for a horizontal plane

The model used is first demonstrated for the direct solar radiation on a horizontal plane. For this method, which uses the solar position algorithm (SPA) (Reda and Andreas, 2008) to calculate the solar radiation on top of the atmosphere (TOA), the general form

TCD
9, 2709–2744, 2015

of the Lambertian cosine law is used:

$$dF = F \cdot \cos\vartheta \cdot d\varpi, \tag{2}$$

where F is the irradiance of the incoming radiation, which is determined by the radiant flux per unit area, ϑ the solar zenith angle and ϖ the solid angle of the sun as seen from the unit area. The irradiance per unit area on TOA is called solar constant, assumed here as $S = 1367\,\mathrm{W\,m^{-2}}$ (Corripio, 2002).

The near-surface incoming direct solar radiation on a horizontal plane (F_{hor}) is given by

$$F_{hor} = S_{terr} \cdot \cos\vartheta_s, \tag{3}$$

where S_{terr} is the near-surface direct solar radiation and ϑ_s the zenith angle of the sun.

Solar radiation is weakened by absorption and scattering between TOA and the surface. This process can be described by the Beer–Lambert–Bouger law (Rontu Carlon et al., 2010), which uses the extinction coefficient $\tilde{\varepsilon}$, depending on the condition of the atmosphere (e.g. aerosols and water vapour content):

$$I = I_0 e^{-\tilde{\varepsilon} d} = I_0 e^{-\frac{\varepsilon}{\cos\vartheta_s}}, \tag{4}$$

where I and I_0 are the intensities of the near surface global and TOA incident solar radiation, respectively and d is the path length in the atmosphere.

To increase the accuracy of the developed model, a linear factor V is introduced to account for the limited spectral range of the instrument (cf. Corripio, 2002, Eq. 3.7 and Kipp & Zonen Manual, 2010) and the varying sun-earth distance is considered. Using Eq. (4) S_{terr} can be written as

$$S_{terr} = \frac{S}{\tilde{r}^2} \cdot V \cdot e^{-\varepsilon \frac{1}{\cos\vartheta_s}}, \tag{5}$$

where $\tilde{r}$ is the ratio of the actual and the mean sun-earth distance. ε and V are two unknown parameters which have to be determined in the first iteration of the correction.

TCD
9, 2709–2744, 2015

Conclusively, in this model the near-surface incoming direct solar irradiance on a horizontal plane can be expressed from Eqs. (3) and (5) as

$$F_{\mathrm{hor}} = \frac{S}{\tilde{r}^2} \cdot V \cdot e^{-\varepsilon \frac{1}{\cos\vartheta_{\mathrm{s}}}} \cdot \cos\vartheta_{\mathrm{s}}. \tag{6}$$

2.2.2 Radiation model for a tilted plane

As most glaciological measurements are conducted on tilted surfaces as shown in (Fig. 2), ϑ in the Lambertian cosine law (Eq. 2), is now $\vartheta_{\mathrm{tilt}}$, the solar incidence angle of a tilted plane, and can be expressed through

$$\cos\vartheta_{\mathrm{tilt}} = \boldsymbol{F}^{\downarrow} \cdot \boldsymbol{n} = \sin\vartheta_{\mathrm{s}} \cos\varphi_{\mathrm{s}} \sin\sigma \cos\gamma + \sin\vartheta_{\mathrm{s}} \sin\varphi_{\mathrm{s}} \sin\sigma \sin\gamma + \cos\vartheta_{\mathrm{s}} \cos\sigma, \tag{7}$$

where $\boldsymbol{n}$ is the n normal vector to the slope, ϑ_{s} is the zenith angle of the sun, φ_{s} the azimuth angle of the sun, σ the tilt and γ the aspect of the slope.

Consequently, the incoming direct radiation on a tilted plane can be derived from Eqs. (6) and (7) as

$$\begin{aligned} F_{\mathrm{tilt}}^{\mathrm{dir}} &= S_{\mathrm{terr}} \cdot \cos\vartheta_{\mathrm{tilt}} = \\ &= \frac{S}{\tilde{r}^2} \cdot V \cdot e^{-\varepsilon \frac{1}{\cos\vartheta_{\mathrm{s}}}} \cdot (\sin\vartheta_{\mathrm{s}} \cos\varphi_{\mathrm{s}} \sin\sigma \cos\gamma + \sin\vartheta_{\mathrm{s}} \sin\varphi_{\mathrm{s}} \sin\sigma \sin\gamma + \cos\vartheta_{\mathrm{s}} \cos\sigma), \end{aligned} \tag{8}$$

To distinguish between a tilted plane and an inclined pyranometer the indices σ_{t}, γ_{t} for “tilt” and σ_{p}, γ_{p} for “pyranometer” are used from here on.

In an idealized model of a measuring system with exactly horizontally levelled sensors, the incoming radiation hits the pyranometer and the tilted surface and is subsequently reflected back to the upper hemisphere as a function of the true snow albedo. In this idealized case using Eq. (1) the irradiance measured with the down-facing sensor can be expressed as

$$F^{\uparrow} = \alpha_{\mathrm{true}} \cdot F_{\mathrm{tilt}}^{\mathrm{dir}}, \tag{9}$$

TCD
9, 2709–2744, 2015
Correction of albedo measurements due to unknown geometry
U. Weiser et al.

Title Page
Abstract | Introduction
Conclusions | References
Tables | Figures
◀ | ▶
Back | Close
Full Screen / Esc
Printer-friendly Version
Interactive Discussion

where $F_{\text{tilt}}^{\text{dir}}$ is defined in Eq. (8) and α_{true} is the true value of the (still unknown) albedo. In this idealized case it is assumed that the total incoming radiation only consists of the direct beam.

The reflected part of the irradiance is measured by the down-facing pyranometer, so the measured albedo can be written as

$$\alpha_{\text{meas}} = \frac{F\uparrow}{F\downarrow} = \frac{\alpha_{\text{true}} \cdot F_{\text{tilt}}^{\text{dir}}}{F\downarrow}. \tag{10}$$

Combining Eqs. (5), (8) and (10), α_{meas} can be simplified to

$$\alpha_{\text{meas}} = \frac{\alpha_{\text{true}} \cdot \frac{S}{\bar{r}^2} \cdot V \cdot e^{-\varepsilon \frac{1}{\cos\vartheta_s}} \cdot \cos\vartheta_{\text{tilt}}}{\frac{S}{\bar{r}^2} \cdot V \cdot e^{-\varepsilon \frac{1}{\cos\vartheta_s}} \cdot \cos\vartheta_s} = \alpha_{\text{true}} \frac{\cos\vartheta_{\text{tilt}}}{\cos\vartheta_s} \tag{11}$$

and the true albedo can be written as

$$\alpha_{\text{true}} = \alpha_{\text{meas}} \frac{\cos\vartheta_s}{\cos\vartheta_{\text{tilt}}}. \tag{12}$$

In Eq. (12) it is assumed that the up-facing pyranometer is levelled horizontally and the reflection of the snow cover is isotropic.

Figure 3 shows the diurnal albedo variations derived with Eq. (11), where a constant true albedo ($\alpha_{\text{true}} = 0.7$) and a constant tilted slope ($\sigma_t = 7°$) are modeled and only the aspect of the slope (γ_t) varies.

To improve the described model it has to be considered that the total incoming radiation measured by the up-facing pyranometer consists not only of a direct beam but also of a diffuse component. Consequently, the total incoming radiation can be split into a direct and a diffuse part (p_{dir} and p_{diff}).

In order to simplify the model, incoming diffuse fluxes over a tilted plane are regarded to be isotropic and equal to incoming diffuse radiation on a horizontal surface. Therefore the incoming radiation on a tilted plane can be split into

$$F_{\text{tilt}} = p_{\text{dir}} F_{\text{tilt}}^{\text{dir}} + p_{\text{diff}} F_{\text{hor}}. \tag{13}$$

Thus the measured albedo is

$$\alpha_{\text{meas}} = \frac{\alpha_{\text{true}}(F_{\text{dir}} + F_{\text{diff}})}{F{\downarrow}} \tag{14}$$

where

$$F_{\text{dir}} = \frac{S}{\tilde{r}^2} \cdot V \cdot e^{-\varepsilon \frac{1}{\cos\vartheta_{\text{s}}}} \cdot p_{\text{dir}} \cos\vartheta_{\text{tilt}} \tag{15}$$

and

$$F_{\text{diff}} = \frac{S}{\tilde{r}^2} \cdot V \cdot e^{-\varepsilon \frac{1}{\cos\vartheta_{\text{s}}}} \cdot p_{\text{diff}} \cos\vartheta_{\text{s}}. \tag{16}$$

The total incoming irradiance can be derived by inserting Eqs. (15) and (16) into Eq. (13) and finally, the true albedo can be written as

$$\alpha_{\text{true}} = \alpha_{\text{meas}} \frac{\cos\vartheta_{\text{s}}}{p_{\text{dir}} \cos\vartheta_{\text{tilt}} + p_{\text{diff}} \cos\vartheta_{\text{s}}}. \tag{17}$$

2.2.3 Radiation model for a tilted slope with an inclined sensor

On a real measuring site, pyranometers are not exactly horizontally levelled. The incoming radiation hits the inclined up-facing pyranometer and the tilted surface, from where it is reflected in an isotropic way into the inclined down-facing pyranometer. However, since we assume that the reflection is completely diffuse, the inclination of the down-facing pyranometer is rendered irrelevant.

TCD
9, 2709–2744, 2015

The true snow albedo can now be derived, considering a tilted slope and an inclined pyranometer by using Eq. (10)

$$\alpha_{\text{true}} = \alpha_{\text{meas}} \frac{\cos \vartheta_{\text{p}}}{\cos \vartheta_{\text{tilt}}} = \alpha_{\text{meas}} \frac{F_{\text{pyr}}}{F_{\text{tilt}}} = \frac{F^{\uparrow}}{F^{\downarrow}} \frac{F_{\text{pyr}}}{F_{\text{tilt}}}, \tag{18}$$

where ϑ_{p} is the inclination angle of the pyranometer, F_{pyr} the incoming irradiance hitting the up-facing pyranometer and F_{tilt} the irradiance hitting the slope.

Figure 5 shows the calculated diurnal albedo using this model with a constant diurnal true albedo ($\alpha_{\text{true}} = 0.7$) for different tilts and inclinations of slope and up-facing pyranometer derived with Eq. (18).

Taking into account the diffuse radiation, F_{pyr} and F_{tilt} have to be split into a direct and a diffuse part analogously to Eqs. (15) and (16). $\cos \vartheta_{\text{p}}$ and $\cos \vartheta_{\text{t}}$ can be derived with tilts and directions of sensor and slope analogously to Eq. (7).

Considering these assumptions, the true albedo can be expressed as

$$\alpha_{\text{true}} = \frac{F^{\uparrow}}{F^{\downarrow}} \frac{p_{\text{diff}} \cdot \cos \vartheta_{\text{s}} + p_{\text{dir}} \cdot \cos \vartheta_{\text{p}}}{p_{\text{diff}} \cdot \cos \vartheta_{\text{s}} + p_{\text{dir}} \cdot \cos \vartheta_{\text{t}}} \tag{19}$$

or, using $p_{\text{dir}} + p_{\text{diff}} = 1$,

$$\alpha_{\text{true}} = \frac{F^{\uparrow}}{F^{\downarrow}} \frac{p_{\text{diff}} \cdot \cos \vartheta_{\text{s}} + (1 - p_{\text{diff}}) \cdot \cos \vartheta_{p}}{p_{\text{diff}} \cdot \cos \vartheta_{\text{s}} + (1 - p_{\text{diff}}) \cdot \cos \vartheta_{\text{t}}}. \tag{20}$$

To correct the albedo with Eq. (20) on clear sky days, the following assumptions and parameters are used:

1. extinction coefficient ε is constant over one day;

2. linear factor V, which represents the ratio between the spectral range of the pyranometer and TOA irradiance, is constant over one day;

3. diffuse reflection of the incoming radiation by the snowcover is assumed to be isotropic and constant over one day (constant snow albedo over one day);
4. fraction of the diffuse to total incoming radiation during a clear sky day is $p_{\mathrm{diff}} \approx 10\,\%$;
5. tilt σ_t and direction γ_t of the slope are constant over one day;
6. tilt σ_p and direction γ_p of the pyranometer are constant over one day.

2.3 Workflow to correct albedo measurements

The determination of tilts and directions of slopes and sensors are accomplished by fitting the model parameters to the measured data (Fig. 6). With these, the albedo values can be corrected.

The described model, including atmospheric parameters, tilts and directions, is now compared to the measured data to evaluate the differences. To find the smallest difference between model and measured data, the method of least squares is used.

2.3.1 Step A: atmospheric parameters for clear sky days

To calibrate the radiation model, the atmospheric model parameters are fitted so as to reduce the residuals between modeled and measured global radiation from BSRN stations SBO and WHW.

In Eq. (6), where the direct incoming radiation on a horizontal plane is derived, ε and V are unknown atmospheric parameters, which need to fit the model to the measured data. The composition of the atmosphere is assumed to be constant during one day over the whole Sonnblick area, where the AWS are drilled into the glaciers and at ZAMG in Vienna, where the Suntracker uses the same coordinates as the measurement setup on the roof.

TCD
9, 2709–2744, 2015

2.3.2 Step B: inclination and direction of the pyranometer

After the atmospheric parameters for one specific day are estimated, the inclinations and directions of the sensors can be derived by using Eq. (13):

$$F_\mathrm{p} = \frac{S}{\tilde{r}^2} \cdot V \cdot e^{-\varepsilon \frac{1}{\cos\vartheta_\mathrm{s}}} \cdot \left((1 - p_\mathrm{diff})\cos\vartheta_p + p_\mathrm{diff}\cos\vartheta_\mathrm{s}\right), \tag{21}$$

where ϑ_p, the solar incidence angle of the pyranometer, can be expressed through the scalar product of the direct sun beam and the normal vector to the pyranometer (Fig. 2), which uses cartesian coordinates analogously to Eq. (7):

$$\begin{aligned} \cos\vartheta_\mathrm{p} &= \boldsymbol{F}^{\downarrow} \cdot \boldsymbol{n} = \\ &= \sin\vartheta_\mathrm{s}\cos\varphi_\mathrm{s}\sin\sigma_\mathrm{p}\cos\gamma_\mathrm{p} + \sin\vartheta_\mathrm{s}\sin\varphi_\mathrm{s}\sin\sigma_\mathrm{p}\sin\gamma_\mathrm{p} + \cos\vartheta_\mathrm{s}\cos\sigma_\mathrm{p}. \end{aligned} \tag{22}$$

The unknown parameters in Eq. (22), σ_p (tilt) and γ_p (direction), are determined by fitting the modeled to the measured data of the up-facing pyranometer with the method of least squares.

This method was used for the AWS on Sonnblick glaciers and for the measurement setup on the roof of ZAMG.

2.3.3 Step C: tilt and direction of the slope

The process to determine the unknown tilts and directions of the slope out of the measured reflected radiation $F^{\uparrow}$ is more complicated because $F^{\uparrow}$ also depends on the unknown albedo of the surface.

It is assumed that the incoming radiation of the slope is directly proportional to the reflected radiation measured by the down-facing pyranometer with the proportionality factor being the yet unknown albedo α_true

$$F^{\uparrow} = \alpha_\mathrm{true} \cdot \cos\vartheta_\mathrm{t}, \tag{23}$$

where ϑ_t is the solar incidence angle on the slope, defined in Eq. (7) as ϑ_{tilt} and illustrated in Fig. 2.

The task now is to find a combination of σ_t (tilt) and γ_t (direction) in such a way that the modeled incoming radiation on the tilted slope and the measured values for $F^{\uparrow}$ only differ by a factor C that should be as constant as possible for one day. First of all, for any combination of σ_t and γ_t, the constant C is calculated as the average over one day:

$$C = \left\langle \frac{F^{\uparrow}}{\cos\vartheta_t} \right\rangle, \tag{24}$$

where $\cos\vartheta_t$ is expressed analogously to Eqs. (7) and (22):

$$\begin{aligned} \cos\vartheta_t &= \boldsymbol{F}^{\downarrow}\cdot\boldsymbol{n} = \\ &= \sin\vartheta_s\cos\varphi_s\sin\sigma_t\cos\gamma_t + \sin\vartheta_s\sin\varphi_s\sin\sigma_t\sin\gamma_t + \cos\vartheta_s\cos\sigma_t. \end{aligned} \tag{25}$$

For every factor C, the method of least squares is used to minimize the difference between modeled and measured reflected radiation:

$$\left(C\cdot\cos\vartheta_t - F^{\uparrow}\right)^2 \longrightarrow \min. \tag{26}$$

This expression is to be minimal for the combination of σ_t and γ_t, for which the proportionality factor C is as constant as possible.

2.3.4 Step D: derive true albedo

Now that all inclinations, tilts and directions are estimated for one day, the true albedo can be derived from the measured data with Eq. (20):

$$\alpha_{true} = \frac{F^{\uparrow}}{F^{\downarrow}}\,\frac{p_{diff}\cdot\cos\vartheta_s + (1-p_{diff})\cdot\cos\vartheta_p}{p_{diff}\cdot\cos\vartheta_s + (1-p_{diff})\cdot\cos\vartheta_t}$$

It is reasonable to use Eq. (20) for an opening angle of the pyranometer of ±80°, so time periods within a flat zenith angle, after sunrise and before sunset, are cut off.

Compared to Steps A–C, where the results are determined by fitting the model to the measured values with the method of least squares, Eq. (20) is only used with measured ($F^{\uparrow}$, $F^{\downarrow}$, p_{diff}) and derived (σ_p, γ_p, σ_t, γ_t) parameters within a certain time interval. The daily mean value as well as the SD of α_{true} are determined.

2.3.5 Step E: derive radiative balance

The effects of corrected albedo values on the shortwave radiative balance are shown by comparing measured and corrected radiative balance.

The shortwave radiative balance is derived as

$$\begin{aligned} \mathrm{SW} &= \mathrm{SW_{in}} + \mathrm{SW_{out}} \\ &= \mathrm{SW_{in}} - \alpha \cdot \mathrm{SW_{in}} \\ &= \mathrm{SW_{in}}(1-\alpha) \end{aligned} \tag{27}$$

In Eq. (27) the albedo α stands for both, α_{meas} and α_{corr}.

3 Results

3.1 Atmospheric parameters

To determine the described atmospheric parameters, the data of the Suntracker are compared to the model of TOA for each location, in this case the roof of ZAMG in Vienna and the Sonnblick Observatory. In both cases the ranges of ε and V are within the same intervals.

The weighted extinction coefficient ranges between $\varepsilon = 0.001$–0.2, which occurs due to several influences, such as temperature, water vapour, aerosols and other meteorological parameters that vary continuously.

TCD
9, 2709–2744, 2015

The ratio between the spectral range of the pyranometer and the irradiance on TOA ranges between $V = 0.8–1$.

3.2 Roof of ZAMG

With the described method, the model was fitted to the measured data (Step B of the workflow to correct albedo measurement) and the mean albedo over one clear sky day was taken.

Subsequently, the pyranometer was intentionally inclined with $\sigma_p \approx 25^\circ$ in westerly direction with $\gamma_p \approx 270^\circ$ over a horizontal concrete plane. As described above, the upper and the lower pyranometer used the same housing and therefore had the same inclination and direction.

The differences between measured and corrected albedo are shown in Fig. 7 and Table 2.

In Fig. 7 (left) the fitted and measured data show an almost constant diurnal albedo on 4 July 2014, where the pyranometer was horizontally levelled. The anomalies shortly after sunrise and before sunset occur due to the cosine error of the up-facing sensor at flat zenith angles.

Figure 7 (right) shows that with an inclined pyranometer the incoming and reflected radiation change unequally, resulting in a modified, wrong surface albedo that is not constant anymore during one clear sky day. After sunrise, the reflected radiation is higher than the incoming radiation which is the result of the westerly inclination of the sensor because the down-facing sensor also receives direct incoming radiation due to the flat zenith angle after sunrise.

In both cases it is apparent that the model that was presumed with a diurnal constant albedo fits the measured data for a horizontal as well as for an inclined sensor. Furthermore, it is reasonable to use the daily mean albedo for both, the measured data and the corrected model, within a zenith angle of $\vartheta_s = \pm 80^\circ$, which is marked by the grey vertical lines.

TCD
9, 2709–2744, 2015
Correction of albedo measurements due to unknown geometry
U. Weiser et al.

After comparing the Suntracker data of several clear sky days all over the year on the WHW and Sonnblick observatory, it is reasonable to assume the diffuse part of the total incoming radiation on a horizontal surface $p_{\text{diff}} \approx 10\,\%$.

The accuracy of the correction method can be demonstrated by comparing the corrected albedo α_{corr} for 4 July with the one for 19 July in Table 2. The deviation between these two is less than 1 %, whereas the deviation between the measured albedo α_{meas} for both days is $\approx 16\,\%$.

3.3 AWS on Sonnblick glaciers

Depending on the direction of the slope and the sensor, the true value of the diurnal mean albedo can either be larger or smaller than the measured one.

In Fig. 7 as well as in Fig. 8 it is apparent that the model can be fitted to the measured data for highly inclined and differently directed sensors and slopes. As the figures show, the model differs from the measured values by approximately 1 % for acceptable zenith angles. The acceptable daily mean albedo within a zenith angle of $\vartheta_s = \pm 80^\circ$ is marked by the gray vertical lines.

The correction for a clear winter day is demonstrated for the southwesterly directed Kleinfleißkees where the corrected diurnal mean albedo is 0.11 less than the measured one. In contrast, the correction for a clear summer day is demonstrated for the northeasterly directed Goldbergkees where the corrected diurnal mean albedo is 0.03 higher than the measured one (see Fig. 8 and Table 3).

These results lead to the conclusion that it depends on the direction of the slope whether the albedo is over- or underestimated.

Furthermore, the absolute value of over- or underestimations in summer months are smaller than in winter months due to a different solar zenith angle.

3.4 Shortwave radiative balance

As shown in the previous sections the directly measured albedo differs from the corrected (true) albedo. This means that the amount of shortwave radiation absorbed by the glacier varies likewise. For example, using data from Table 3, directly measured values for Kleinfleißkees indicate that 14 % of the incoming shortwave radiation SW_{in} are absorbed by the glacier. On the other hand, the corrected values show that 25 % of the incoming shortwave radiation are absorbed.

The correction of the radiative balance using Eq. (27) is demonstrated in Fig. 10 for the two sample days, where on 5 March 2011 on Kleinfleißkees the corrected radiative balance SW_{corr} is roughly 55 % higher than the measured one SW_{meas} and on 27 June 2011 on Goldbergkees SW_{corr} is roughly 7 % smaller than SW_{meas}.

Over the year 2011 the corrected radiative balance SW_{corr} on Kleinfleißkees ≈ 8 % higher than the measured one (SW_{meas}). On Goldbergkees the corrected radiative balance SW_{corr} is ≈ 6 % smaller than the measured one. The relatively small absolute values of the corrections result from the fact that there are more cloudy than clear sky days over the year.

4 Discussion

The described method can be used on clear sky days and on days with a short period of clear sky, with a minimum of 2–3 h. On these days, the clouded part has to be cut off when fitting the model to the measured data. Also shadows of nearby mountains have to be cut off to use just the clear sky part with direct incoming radiation. The advantage of this method is that it is not limited to completely clear sky days, which are relatively rare in mountainous areas.

The differing optical path length through the atmosphere due to the curvature of the earth has to be considered, especially when the zenith angle is flat at sunrise and sunset, hence it is reasonable to neglect these time intervals.

TCD
9, 2709–2744, 2015

When the inclinations of the sensors are too large, the down-facing sensor receives parts of the incoming radiation after sunrise or before sunset, depending on the direction. For these days a correction for the albedo is less useful because incoming and reflected radiation are not clearly separated any more.

On days after snowfall it can happen that the up-facing sensor is still covered with snow and after melting periods there are water drops on the down-facing sensor.

Sometimes the solar panel attached to the AWS is covered with snow, so the self-contained power supply is not guaranteed. Especially in winter months the AWS cannot take measurements for longer time periods due to their isolated locations.

The atmospheric parameters, as well as tilts and directions of slopes and sensors have to be calibrated every day which is very time consuming and cannot be fully automated due to different cut-offs. If there is no reference measurement nearby, this method cannot be applied. As a further consequence, an improvement of this method would be to use a model that finds atmospheric parameters without a reference measurement, using meteorological parameters, such as aerosol concentration, water vapour, temperature, etc.

To minimize tilt errors in albedo measurement, the sensor can be adjusted parallel to the slope, such that the incident radiation is identical for both. Ideal measurement setups are over flat surfaces with horizontally levelled sensors, which is difficult in mountainous areas on glaciers.

5 Conclusions

Directly measured snow albedo variations on clear sky days can be relatively high due to tilted slopes and inclined pyranometers, hence it is challenging to determine a diurnal mean albedo from directly measured data. The tilts and directions of sensors and slopes were unknown and it was difficult to make permanent manual reference measurements due to the isolated location of the measuring sites. To compensate for

TCD
9, 2709–2744, 2015

this problem, a model was developed with the aim to allow accurate estimations of measurement site's tilts and orientations of slope and sensors.

For this model, atmospheric parameters are determined using a nearby horizontally levelled pyranometer to find the difference between TOA and near surface incoming shortwave radiation. With these parameters, the model is fitted to the measured data. The results of these fitting procedures are tilts and directions of both, the sensors and the slopes.

With these tilts and directions, the true albedo can be derived from the measured data. Especially in winter months (September to June) and in polar areas, where the zenith angle of the direct sun beam is flat, the differences are relatively high.

To prove this method, an experimental measurement was taken for a horizontal concrete surface with a pyranometer with and without inclination. The results show a different diurnal mean albedo. The atmospheric parameters, the inclination and the direction of the sensor were determined with the described method. Furthermore, the true albedo was derived and compared to the diurnal mean albedo measured by a horizontally levelled pyranometer over the same surface. The difference between these values was less than 1 %, whereas the difference between the directly measured values by an inclined pyranometer was ≈ 16 %.

Consequently, the difference between the directly measured and the corrected radiative balance can be significant on single clear sky days especially with a flat zenith angle.

Acknowledgements. This work was financed by the FEMtech programme of the Österreichische Forschungsförderungsgesellschaft (FFG) and the Central Institute for Meteorology and Geodynamics (ZAMG).

References

Allen, R., Trezza, R., and Tasumi, M.: Analytical integrated functions for daily solar radiation on slopes, University of Idaho Research and Extension Center, United States, Agr. Forest Meteorol., 139.1, 55–73, 2006. 2712

Amsys: Neuartige Neigungssensoren für die präzise Winkelmessung, Die elektronische Wasserwaage, available at: http://www.amsys.de/sheets/amsys.de.aan514_3.pdf, last access: 27 January 2015, 2012.

Corripio, J.: Modelling the engergy balance of high altitude glacierised basins in the Central Andes, PhD thesis, University of Edinburgh, UK, 2002. 2716

Dirmhirn, I. and Eaton, F.: Some characteristics of the albedo of snow, J. Appl. Meteorol., 14, 375–379, 1975. 2711

Ineichen, P., Perez, R., and Seals, R.: The importance of correct albedo determination for adequately modeling energy received by tilted surfaces, Sol. Energy, 39, 301–305, doi:10.1016/S0038-092X(87)80016-6, 1987. 2712

Kipp & Zonen: Instruction Manual, CNR4 Net Radiometer, Campbell Scientific, Inc., Kipp & Zonen B. V., AM Delft, The Netherlands 2010.

Landry, C., Painter, T., Barrett, A., and Cassidy, M.: Toward standardization in Methods and Techniques for Measuring and Monitoring Snowcover Albedo, 10 December 2007, San Francisco, CA, USA, American Geophysical Union, Fall Meeting 2007, abstract #GC32A-03, 2007. 2711

Mannstein, H.: The interpretation of albedo measurements on a snow covered slope, Arch. Met. Geoph. Biocl., Ser. B., 36, 73–81, 1985. 2712

Muneer, T.: Solar Radiation and Daylight Models, 2nd Edn., Elsevier Butterworth-Heinemann, Oxford, 1997. 2711

Oerlemans, J.: The Microclimate of Valley Glaciers, Igitur, Utrecht University, The Netherlands, 138 pp., 2010. 2711, 2712

Reda, I. and Andreas, A.: Solar position algorithm for solar radiation applications, National Renewable Energy Laboratory (NREL), Golden, CO, USA, Technical Rep. NREL/TP-560-34302, 56 pp., 2008. 2715

Rontu Carlon, N., Papanastasiou, D. K., Fleming, E. L., Jackman, C. H., Newman, P. A., and Burkholder, J. B.: UV absorption cross sections of nitrous oxide (N_2O) and carbon

TCD
9, 2709–2744, 2015

Correction of albedo measurements due to unknown geometry

U. Weiser et al.

tetrachloride (CCl_4) between 210 and 350 K and the atmospheric implications, Atmos. Chem. Phys., 10, 6137–6149, doi:10.5194/acp-10-6137-2010, 2010. 2716
Santamouris, M.: Environmental Design of Urban Buildings: an Integrated Approach, Earthscan, UK, 2006. 2715
Schaaf, C., Li, X., and Strahler, A.: Topographic effects on bidirectional and hemispherical reflectances calculated with a geometric-optical canopy model, IEEE T. Geosci. Remote, 32, 1186–1193, 1994. 2712
Sicart, J., Ribstein, P., Wagnon, P., and Braunstein, D.: Clear-sky albedo measurements on a sloping glacier surface: A case study in the Bolivian Andes, J. Geophys. Res., 106, 31729–31737, doi:10.1029/2000JD000153, 2001. 2711
Warren, S.: Optical properties of snow, Rev. Geophys., 20, 67–89, doi:10.1029/RG020i001p00067, 1982
Weiser, U.: Methode zur Korrektur von Neigungsfehlern bei der zeitlichen Albedo-Messung an wolkenlosen Tagen, MSc thesis, University of Vienna, Vienna, Austria, 2012. 2712

Table 1. Geographic latitude ϕ and longitude ϑ, altitude and direction of the used measurement stations.

	SBO	FLK	GOK	WHW
ϕ	12°57′28″	12°56′42″	12°57′50″	16°21′23″
ϑ	47°3′14″	47°3′15″	47°2′38″	48°14′55″
altitude	3111 m	2829 m	2678 m	198 m
direction		SW	NE	

TCD
9, 2709–2744, 2015

Table 2. Results of measured and corrected inclinations and directions and daily average albedo at WHW on 4 and 19 July 2014.

	4 Jul 2014	19 Jul 2014
σ_p	$0.3^\circ \pm 0.0003^\circ$	$24.0^\circ \pm 0.024^\circ$
γ_p	$5.0^\circ \pm 0.025^\circ$	$265.0^\circ \pm 1.325^\circ$
$\sigma_{p(meas)}$	$1.27^\circ \pm 0.01^\circ$	$23.33^\circ \pm 0.12^\circ$
$\gamma_{p(meas)}$	$170.44^\circ \pm 0.85^\circ$	$264.32^\circ \pm 1.32^\circ$
α_{meas}	0.1791 ± 0.0063	0.2083 ± 0.0696
α_{corr}	0.1789 ± 0.0064	0.1773 ± 0.0082

TCD
9, 2709–2744, 2015

Table 3. Results of measured and corrected inclinations and directions and daily average albedo on Kleinfleißkees on 5 March 2011 and on Goldbergkees on 27 June 2011.

	FLK, 5 Mar 2011	GOK, 27 Jun 2011
σ_t	$10.57^\circ \pm 0.05^\circ$	$13.51^\circ \pm 0.11^\circ$
γ_t	$225.00^\circ \pm 5.60^\circ$	$41.43^\circ \pm 4.93^\circ$
σ_p	$4.72^\circ \pm 0.11^\circ$	$3.93^\circ \pm 0.08^\circ$
γ_p	$247.62^\circ \pm 3.37^\circ$	$9.68^\circ \pm 0.68^\circ$
$\sigma_{p(meas)}$	$4.29^\circ \pm 0.02^\circ$	$7.77^\circ \pm 0.39^\circ$
$\gamma_{p(meas)}$	$305.43^\circ \pm 1.53^\circ$	$52.54^\circ \pm 0.26^\circ$
α_{meas}	0.86 ± 0.07	0.51 ± 0.06
α_{corr}	0.75 ± 0.01	0.54 ± 0.01

TCD
9, 2709–2744, 2015

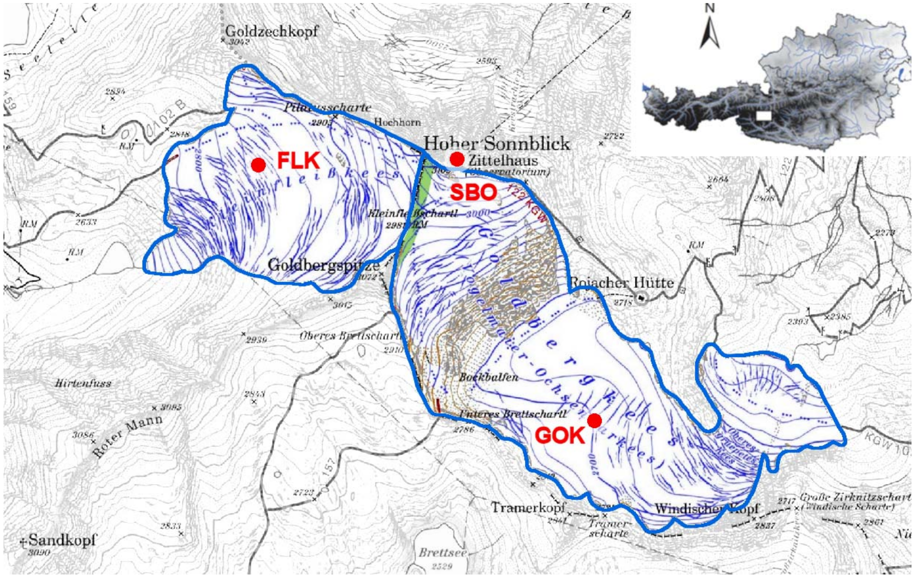

Figure 1. Map of Sonnblick area (taken from Alpenvereinskarten digital 2007, Vers. 2.0.9.0, DAV (Munich), ÖAV (Innsbruck)). The red marks indicate the positions of the AWS and SBO.

TCD
9, 2709–2744, 2015

Correction of albedo measurements due to unknown geometry

U. Weiser et al.

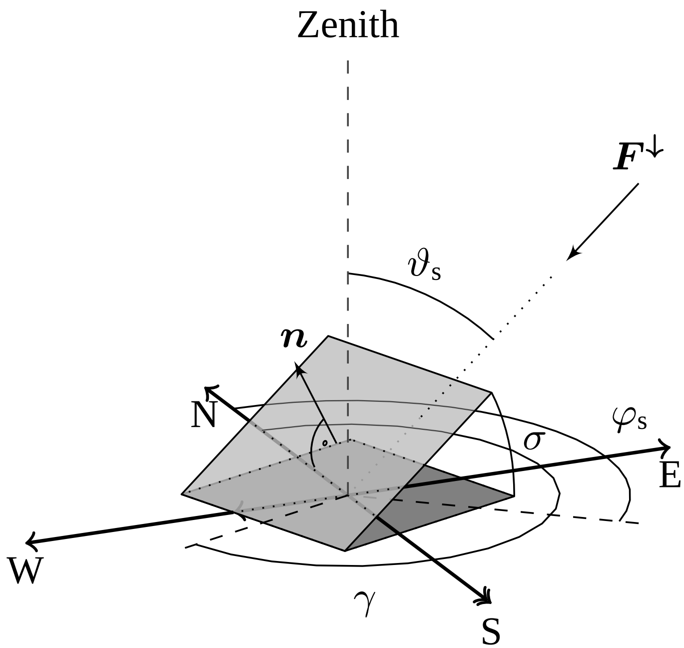

Figure 2. Geometric account of a tilted surface.

TCD
9, 2709–2744, 2015

Correction of albedo measurements due to unknown geometry

U. Weiser et al.

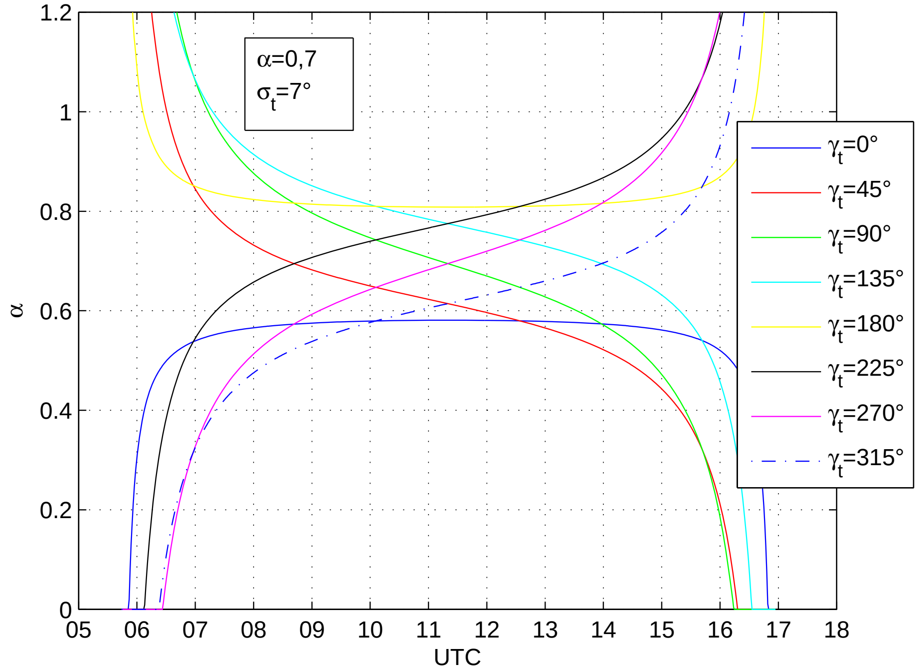

Figure 3. Diurnal variations of albedo with a constant true albedo, a constant tilt of the slope but differing aspects.

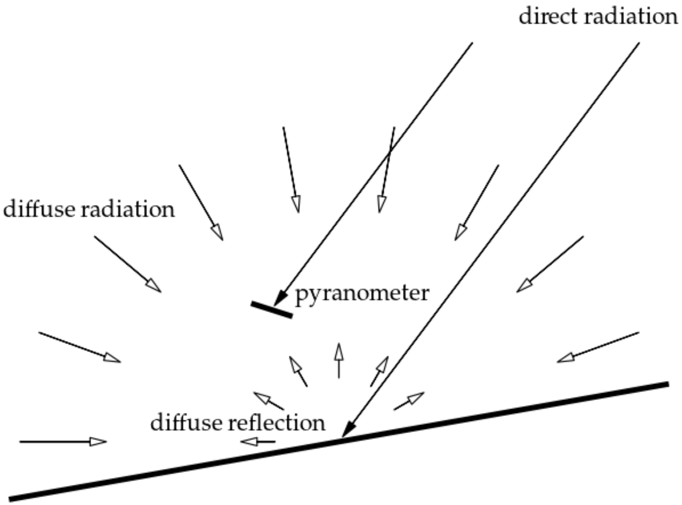

Figure 4. Isotropic reflection from a tilted slope with an inclined pyranometer.

TCD
9, 2709–2744, 2015

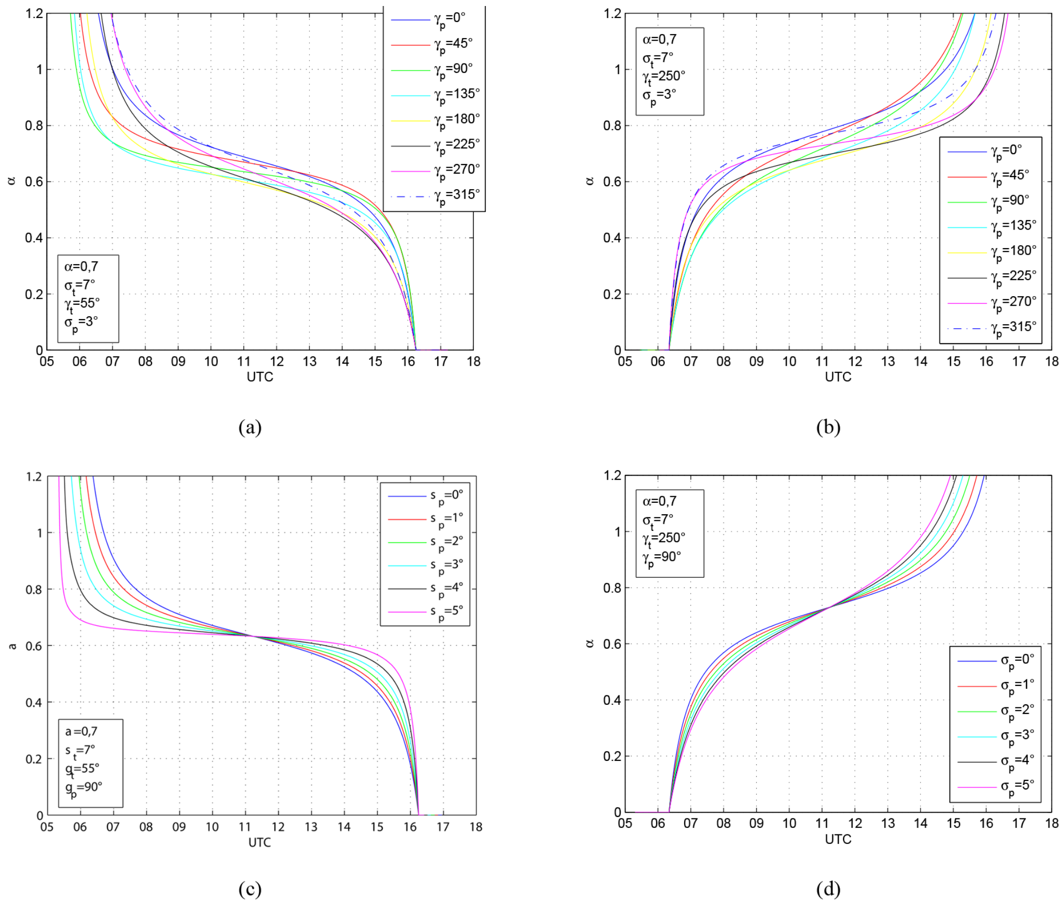

Figure 5. Calculated albedo with a constant diurnal true albedo for (**a** and **b**) differently oriented (γ_p) and (**c** and **d**) inclined (σ_p) pyranometers, different tilted (σ_t) and directed (γ_t) slopes.

TCD
9, 2709–2744, 2015

Title Page
Abstract | Introduction
Conclusions | References
Tables | Figures
◀| |▶
◀ ▶
Back | Close
Full Screen / Esc
Printer-friendly Version
Interactive Discussion

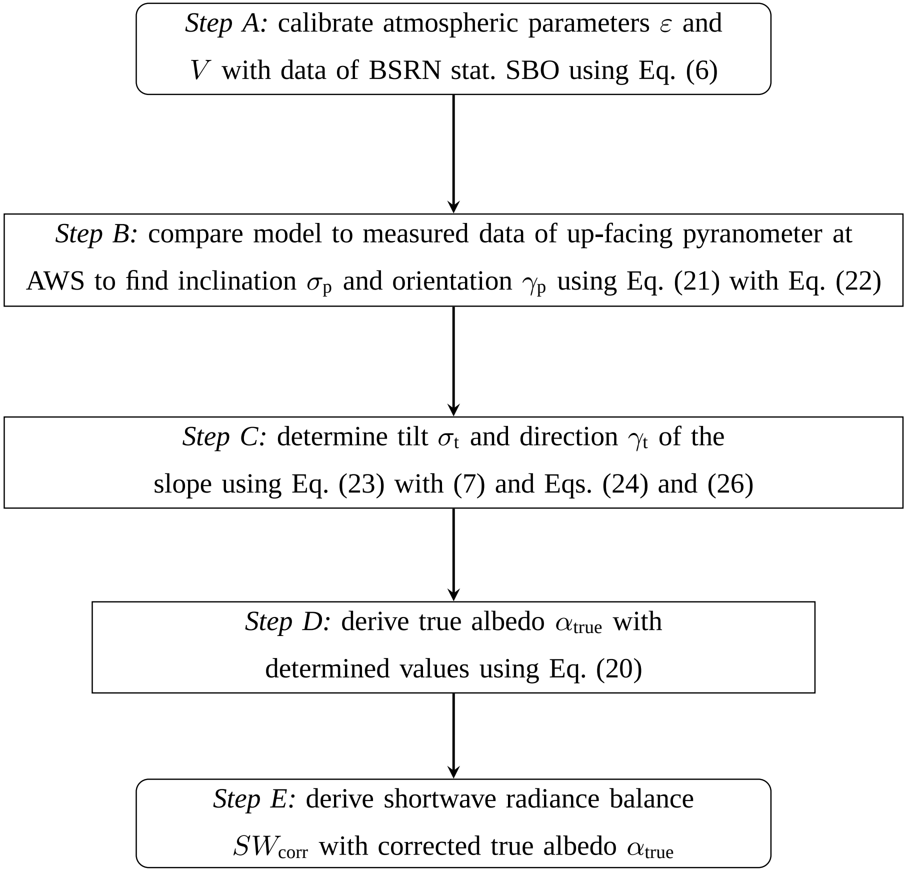

Figure 6. Workflow to correct daily albedo values.

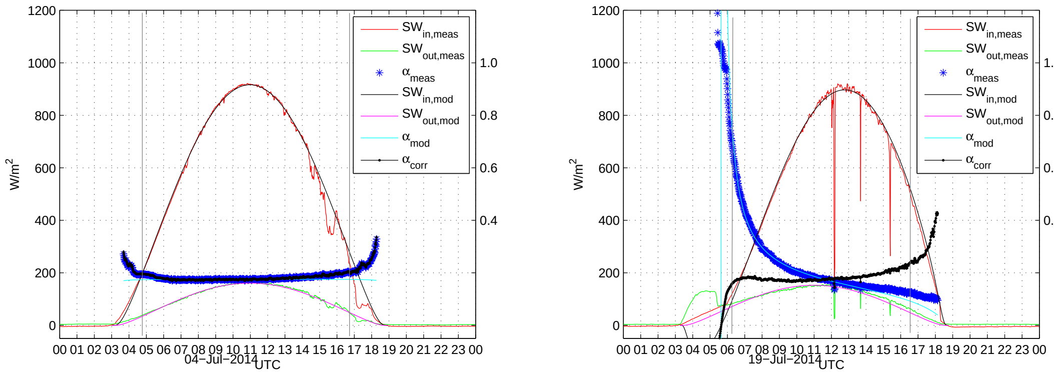

Figure 7. Measured, modeled and corrected SW_{in}, SW_{out} and α with a horizontally levelled (left) and an intentionally inclined pyranometer (right) at WHW for two days in July 2014.

TCD
9, 2709–2744, 2015

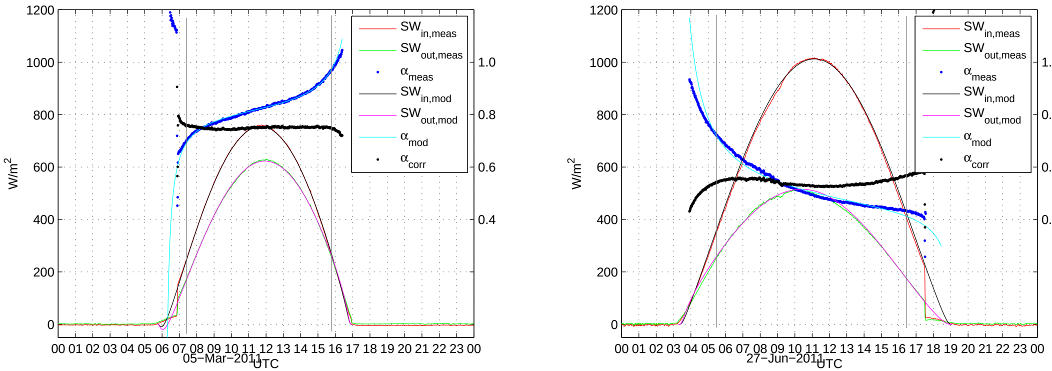

Figure 8. Directly measured (blue dots), modelled (cyan) and corrected (black dots) albedo calculated from data of an inclined pyranometer and a tilted slope at the location of the AWS on Kleinfleißkees on 5 March 2011 (left) and Goldbergkees on 27 June 2011 (right).

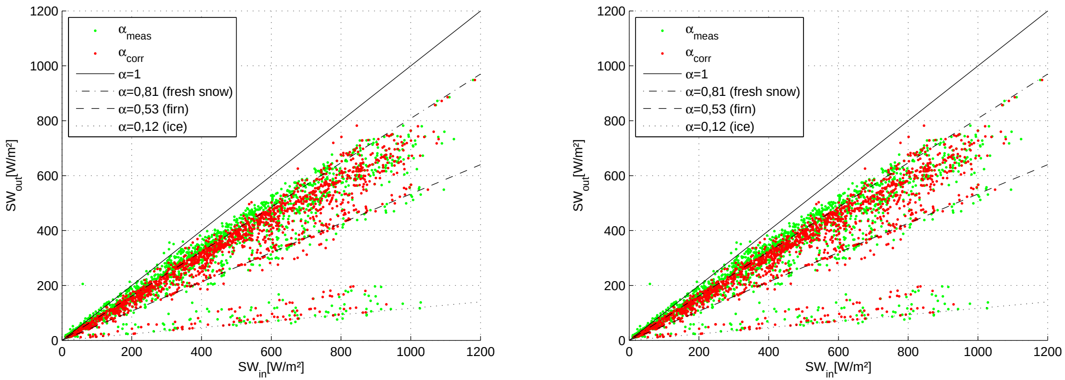

Figure 9. Measured (green) and corrected (red) albedo values on Kleinfleißkees (left) and Goldbergkees (right) for all the year 2011.

TCD
9, 2709–2744, 2015

Correction of albedo measurements due to unknown geometry

U. Weiser et al.

TCD
9, 2709–2744, 2015

Correction of albedo measurements due to unknown geometry

U. Weiser et al.

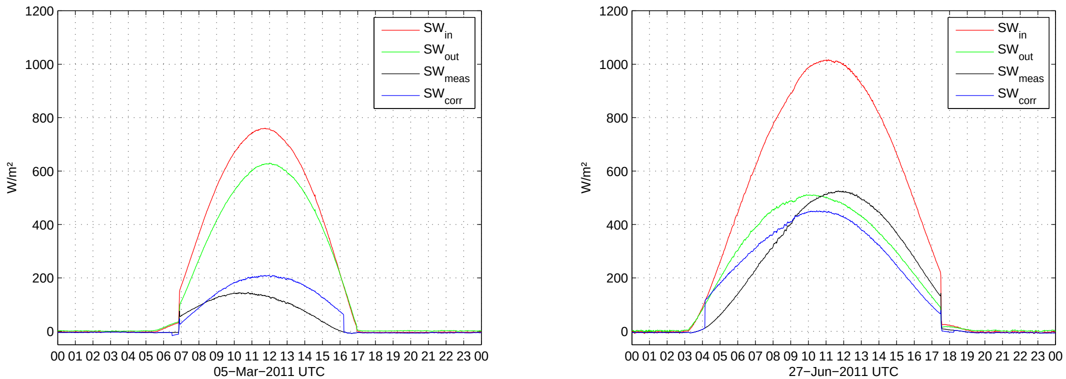

Figure 10. Measured (SW$_{meas}$) and corrected (SW$_{corr}$) shortwave radiative balance on Kleinfleißkees on 5 March 2011 (left) and on Goldbergkees on 27 June 2011 (right).